A Risk-Averse Adaptive Stochastic Optimization Method for Transactive Energy Management of a Multi-Energy Microgrid

Yunyang Zou, *Student Member, IEEE*, Yan Xu, *Senior Member, IEEE*, and Cuo Zhang, *Member, IEEE*

***Abstract*—This paper proposes a new energy management method for a multi-energy microgrid (MEMG) which supplies both electrical and thermal energies. Based on the transactive energy (TE) concept, the problem is formulated as a Stackelberg game-theoretic bi-level optimization model. The MEMG operator optimizes the energy scheduling and pricing strategies at the upper level, and the industrial, commercial and residential agents optimize their energy trading strategies at the lower level. The equivalent single-level mixed-integer linear program (MILP) reformulation is then derived for computational tractability. To coordinate the strategies made in the day-ahead and intra-day energy markets, an adaptive stochastic optimization (SO) approach is adopted, by which a day-ahead stochastic MILP and an intra-day deterministic model are formed. Furthermore, the conditional value-at-risk (CVaR) measure is incorporated in the day-ahead stage for risk aversion of the MEMG operator towards uncertainties. To solve the models, an adaptive Progressive Hedging (PH) algorithm is developed to decompose the day-ahead stochastic MILP into multiple scenario-based subproblems which can be solved in parallel, and an outer approximation (OA) algorithm is adopted in the intra-day stage to linearize the bilinear objective function. Finally, the simulation results verify the effectiveness of the proposed energy management method and the efficiency of the solution algorithms.**

***Index Terms*—Transactive energy, multi-energy microgrid, stackelberg game, adaptive stochastic optimization, risk averse.**

NOMENCLATURE

A. Acronyms

BS(C/D)	Battery storage (charging/discharging).
DER	Distributed energy resource.
ESS	Energy storage system.
EU	Energy user.
MEMG	Multi-energy microgrid.
TS(C/D)	Thermal storage (charging/discharging).

B. Sets and Indices

N_T/t	Set/Index of time slots.
N_J/j	Set/Index of DGs.
N_I/i	Set of exogenous networks ($i = 0$), residential ($i = 1$), commercial ($i = 2$) and industrial ($i = 3$) agents.

C. Parameters

$\kappa^{(\cdot)}$	Unit operating cost.
$\lambda_{0,t}^{elec}/\lambda_{0,t}^{thm}$	Prices for selling electrical/thermal energy to exogenous networks in the day-ahead market.
$\lambda_{exo,t}^{elec}/\lambda_{exo,t}^{thm}$	Prices for buying electrical/thermal energy from exogenous networks in the day-ahead market.
$\Lambda_{0,t}^{elec/thm}$	Prices for selling electrical/thermal energy to exogenous networks in the intra-day market.
$\Lambda_{exo,t}^{elec/thm}$	Prices for buying electrical/thermal energy from exogenous networks in the intra-day market.
P_t^{PV}/P_t^{WT}	Electrical power outputs of a PV/WT.
$E_0^{BS/TS}$	Initial energy stored in a BS/TS.
$E^{BS/TS,rate}$	Rated capacity of a BS/TS.
η^{CCHP}	Thermal-to-electrical ratio of a CCHP unit.
η^{BSC}/η^{BSD}	Charging/discharging efficiency of a BS.
η^{TSC}/η^{TSD}	Charging/discharging efficiency of a TS.
$\tau^{BS/TS}$	Decay rate of a BS/TS.
$P_{i,t}^{exp}/\theta_{i,t}^{exp}$	Expected electrical energy demand and indoor temperature of EU agent *i*.
$\alpha_{i,t}/\beta_{i,t}$	Unit discomfort cost for electrical/thermal energy demand deviation of EU agent *i*.
γ_i	Minimum daily demand ratio of EU agent *i*.
C_i^{air}	Heat capacity of the air.
R_i^T	Thermal resistance of building shells.
$\theta_{i,t}^{am}$	Ambient temperature.
$\chi_{\min/\max}^{BS/TS}$	Minimal/maximal state of charge of a BS/TS.
$(\cdot)^{\min/\max}$	Minimal and maximal limits.

D. Variables

$\lambda_{i,t}^{elec}/\lambda_{i,t}^{thm}$	Electrical/thermal trading prices between the MEMG operator and EU agent i ($i \in N_I \backslash 0$) in the day-ahead market.

Manuscript received 22 August 2022; revised 7 December 2022; accepted 20 January 2023. Date of publication 26 January 2023; date of current version 21 June 2023. The work of Yan Xu was supported in part by the National Research Foundation, Prime Minister's Office, Singapore, and in part by the Energy Market Authority through the Exploiting Distributed Generation Programme and administrated by the EDGE Programme Office under EDGE Programme under Grant NRF2014EWT-EP003-008. Paper no. TSTE-00871-2022. *(Corresponding author: Yan Xu.)*

Yunyang Zou and Yan Xu are with the School of Electrical and Electronic Engineering, Nanyang Technological University, Singapore 639798 (e-mail: yunyang001@e.ntu.edu.sg; xuyan@ntu.edu.sg).

Cuo Zhang is with the School of Electrical and Information Engineering, The University of Sydney, Sydney, NSW 2006, Australia (e-mail: cuo.zhang@sydney.edu.au).

Color versions of one or more figures in this article are available at https://doi.org/10.1109/TSTE.2023.3240184.

Digital Object Identifier 10.1109/TSTE.2023.3240184

$P_{i,t}^{elec}/P_{i,t}^{thm}$	Electrical/thermal trading quantities the MEMG operator sells to entity i in the day-ahead market.
$\Lambda_{i,t}^{elec/thm}$	Electrical/thermal trading prices between the MEMG operator and EU agent i in the intra-day market.
$\Delta P_{i,t}^{elec/thm}$	Electrical/thermal trading quantities the MEMG operator sells to (>0) or buys from (<0) entity i in the intra-day market.
$P_{j,t}^{DG}$	Electrical power output of DG j.
$P_{t}^{CCHP,el/th}$	Electrical/thermal power output of a CCHP unit.
P_{t}^{BSC}/P_{t}^{BSD}	Charging/discharging power of a BS.
P_{t}^{TSC}/P_{t}^{TSD}	Absorbing/releasing power of a TS.
E_{t}^{BS}/E_{t}^{TS}	Stored energy in a BS/TS.
$P_{i,t}^{el,e}/P_{i,t}^{th,e}$	Electrical/thermal trading quantities agent i buys from exogenous networks in the day-ahead market.
$\Delta P_{i,t}^{el/th,e}$	Electrical/thermal trading quantities agent i buys from (>0) or sells to (<0) exogenous networks in the intra-day market.
$P_{i,t}^{ed}/\theta_{i,t}^{td}$	Actual electrical energy demand and indoor temperature of EU agent i.
$P_{i,t}^{td}$	Actual thermal energy demand of EU agent i.

I. Introduction

A. Background and Motivation

A MULTI-ENERGY microgrid (MEMG) integrates distributed generation units such as photovoltaic (PV) system, wind turbine (WT), and combined cooling heat and power (CCHP) units to simultaneously provide multiple energy supplies to customers for enhanced energy efficiency [1]. The MEMG can be deployed at district level (e.g., community, building, industrial park, and even distribution network) [2], together with flexible loads, such as demand response program electric vehicles (EVs) and thermostatically controlled loads (TCLs).

B. Literature Survey

Significant research efforts on multi-energy management have been devoted in the literature, but most of them mainly focus on the supply-side energy management and oversimplify the demand-side management. In [3], the MEMG operator treats power demands as stochastic parameters and directly manage thermal demands without compromising customers' comfort. In [4], the multi-energy building operator dispatches both electrical and thermal loads through direct-load-control (DLC). In [5], the MEMG operator treats the electrical power loads as stochastic parameters and proposes a risk-averse energy management method, but manages thermal loads through DLC. Recently, the concept of transactive energy (TE) has been proposed, which is defined as a set of economic and control mechanisms allowing the dynamic balance of supply and demand across the entire electrical infrastructure with price as a key operational parameter [6]. As an indirect control signal, an appropriate price can lead to desired demand-side response, thereby achieving an expected energy supply-demand balance. Besides, it can further reduce the local MEMG's reliance on exogenous networks. Hence, by integrating a pricing scheme, the demand-side management can be promoted and an efficient transactive energy management can be achieved.

In general, there are three main methods for designing pricing schemes for transactive energy management, including auction mechanism [7], [8], [9], dual price [10], [11], [12] and game theory [13], [14], [15], [16], [17], [18], [19]. Ref. [7] reports a double-auction peer-to-peer energy trading scheme within a distribution grid. In [10], the market clearing mechanism is designed based on a dual decomposition approach for a local energy network. In [13], the energy scheduling and trading decisions of multi-carrier energy hubs are optimized based on Nash bargaining theory. In [14], the operators in a multi-energy industrial park use Stackelberg game theory to determine the compensation prices for peak load shifting. A more detailed literature review and comparison of the above three pricing methods can be found in our review paper [20]. Among them, the game theory can effectively capture the complicated strategic interactions among diverse stakeholders, which attracts wide attention for designing transactive energy management.

Furthermore, since the microgrid operator generally has a strategic advantage in a local energy market and consumers can only make their decisions based on operator's decision, Stackelberg game is especially effective under such cases. For instance, [15] develops a Stackelberg game-theoretical bi-level model to determine the energy dispatch and pricing for maximizing the owner's revenue, who owns and shares the solar PV and energy storage in an apartment building. In [16], an electrical-gas-thermal energy sharing mechanism is established based on Stackelberg game, with the aim of maximizing the energy hub operator's profit. Ref. [17] formulates the transactive energy management of a MEMG with bidirectional electricity/heat prices as a Stackelberg game model. Aiming at maximizing the energy service provider's profit in a regional integrated energy system, a day-ahead energy pricing scheme with associated energy management is expressed as a bilevel Stackelberg game model in [18]. Nonetheless, it should be noticed that the abovementioned works all ignore the underlying impacts of uncertainties, e.g., stochastic renewable power generation.

To address the operational uncertainties for power system optimization, several methods have been proposed in the literature, such as stochastic optimization (SO), robust optimization [21], interval optimization [22] and chance constrained programming [23]. To sufficiently utilize the probabilistic information of uncertainties while maintaining a reasonably computational tractability, SO approaches have been widely applied to transactive energy management: Ref. [11] proposes a transactive energy supported operation framework for interconnected MEMGs. In [8], a Vickrey auction theory and a Stackelberg game are jointly applied in the H_2 pricing mechanism for maximizing a hybrid-renewable-to-H_2 provider's profit. In [19], the energy management of a price-maker storage system is formulated as a stochastic bi-level model. However, the above day-ahead energy management decisions derived by a single-stage SO can only guarantee the expectation is optimal over all scenarios generated

TABLE I
COMPARISON BETWEEN THIS PAPER AND THE EXISTING WORKS

Ref.	Multi-energy management	Energy transaction	Uncertainty handling	Multiple timescale coordination	Risk aversion
[3, 4, 21, 22]	✓	×	✓	✓	×
[5, 23]	✓	×	✓	✓	✓
[7, 10, 15]	×	✓	×	×	×
[8, 11]	✓	✓	✓	×	×
[13, 14, 16-18]	✓	✓	×	×	×
[12, 19]	×	✓	✓	×	×
[9]	×	✓	✓	✓	×
[24]	✓	✓	✓	✓	×
This paper	✓	✓	✓	✓	✓

based on the day-ahead forecasts. Hence, as the uncertainties are realized gradually, an intra-day energy management decision should also be provided for maintaining optimal energy management.

In this regard, a two-stage energy management framework is needed to coordinate the day-ahead and intra-day decisions. Aiming at minimizing the operation costs, [9] presents a two-stage SO energy management model to coordinate energy trading and generation scheduling for a microgrid. Ref. [24] proposes a two-stage hybrid stochastic and robust model, maximizing the microgrids' profits in the day-ahead market and minimizing the imbalance cost in the real-time balancing market, but it lacks specifical pricing schemes. To efficiently solve the large-scale model, the scenario reduction is usually implemented in SO, which however may disregard the low-probability-high-impact scenarios [5]. As a result, it may lead to a large deviation from the expected profit/cost under some unfavorable scenarios. Generally, most of microgrid operators are risk averse towards uncertainties, which means they do not hope to suffer such a large deviation from the expected value. Therefore, a proper risk measurement index should be considered and incorporated into the day-ahead SO model for optimizing the day-ahead energy management decisions. It is also worth noting that the day-ahead problems in the abovementioned works are all formulated as a stochastic mixed-integer program (MIP) model and directly solved by commercial solvers. However, such models, especially with a large number of integer variables, have a heavy computational burden, which is still intractable for the cutting-edge solvers. To this end, a decomposition algorithm is highly desirable to reduce the computation difficulty of stochastic MIP problems.

C. Contribution of This Paper

To fill the research gaps, this paper proposes a new risk-averse two-stage transactive energy management method for a MEMG to optimize the day-ahead and intra-day energy scheduling and pricing strategies. The differences between the existing works and this paper are compared in Table I. The proposed method and its technical features are summarized as follows.

1) According to different user behaviors, consumers are categorized into industrial, commercial and residential energy users (EUs) in this paper. Unlike most existing works that mainly focus on the MEMG supply-side energy management and oversimplify the demand-side management, this paper formulates the transactive energy management of a MEMG as a Stackelberg game-based bi-level model, in which the MEMG operator and different EUs are effectively interacted.
2) A two-stage transactive energy management framework for the MEMG is designed, and an adaptive SO approach is proposed to coordinate the day-ahead and intra-day transactive energy management decisions considering uncertainties of renewable generation and ambient temperature. Moreover, a conditional value-at-risk (CVaR) measure is applied in the day-ahead stage for risk aversion of the MEMG operator towards the uncertainties.
3) To reduce the computation difficulty of the multi-scenario stochastic MIP problem, an adaptive Progressive Hedging (PH) algorithm is developed, which can decompose the day-ahead stochastic mixed-integer linear program (MILP) into multiple scenario-based subproblems to be solved in parallel. Besides, an outer approximation (OA) algorithm is used to solve the intra-day bilinear problem without introduction of binary variables. Both algorithms achieve significant improvement in computation efficiency.

The rest of the paper is organized as follows. The proposed MEMG energy management framework is described in Section II. Section III firstly presents the deterministic joint multi-energy scheduling and trading formulation for a MEMG based on a Stackelberg game. Then, a risk-averse adaptive SO approach is proposed in Section IV, by which the deterministic model is extended to a day-ahead risk-averse stochastic model and an intra-day deterministic model. Section V gives two iterative algorithms for solving the day-ahead and intra-day optimization models, respectively. Case studies are conducted in Section VI, and the conclusions are drawn in Section VII.

II. PROPOSED TRANSACTIVE ENERGY MANAGEMENT FRAMEWORK FOR A MEMG

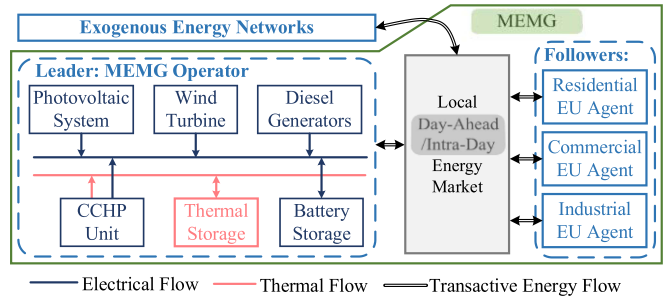

Fig. 1. Structure of the MEMG considering transactive energy.

The proposed transactive energy management framework for a MEMG is illustrated in Fig. 1. The local energy market within the MEMG involves four participants. The MEMG operator is responsible for scheduling all the physical DER units, including a CCHP unit, diesel generators (DGs), renewable energy generation units and ESSs. Meanwhile, the MEMG operator also determines the appropriate energy trading prices for desired demand-side response. Three agents are introduced to represent the aggregated industrial, commercial, and residential EUs, respectively. To meet the thermal and electrical demands, the EU agents transact with the MEMG operator through the local energy market. The local energy market as a non-monopoly market also allows all the MEMG participants to trade energies directly with the exogenous energy networks (i.e., utility grid and district thermal network). The selling/ buying prices for trading energy with the exogenous networks are given by time-of-use (TOU) pricing scheme in this paper, and thus treated as known parameters. Note that other pricing schemes for the exogenous networks can also be applied.

In a two-stage framework, the local day-ahead and intra-day energy markets are considered. They allow EU agents to transact with the MEMG operator, which can greatly facilitate the local power balance and reduce the MEMG's reliance on the exogenous energy networks. In the day-ahead energy market, the MEMG operator uses the day-ahead probabilistic predictions of the uncertainties (i.e., renewable generation and ambient temperature) to determine the 24-hour energy scheduling and pricing strategies for daily profit maximization. Based on the prices released by the MEMG operator, the EU agents, as price takers, optimize their day-ahead energy procurement commitments considering the trading cost and comfort level. Through the internal energy trading, the local energy generation can be consumed locally as much as possible. Since reselling procured energy cannot make any profits in a non-monopoly market, the MEMG operator (as an energy producer) only sells energy to others while the EU agents (as energy consumers) just buy energy from others in the day-ahead energy market.

The intra-day energy market is an hourly-ahead market. In this market, the updated hourly-ahead point predictions of the uncertain parameters are used. To address the hourly-ahead power imbalance caused by uncertainties, the power output of the CCHP unit is scheduled in every hour. Considering the relatively slow response of DGs and more degradation of ESSs after frequent changing/discharging, the day-ahead schedules on ESSs and DGs will remain unchanged in this intra-day stage. Other than rescheduling the CCHP unit, the MEMG operator also releases newly hourly-ahead prices in this intra-day market to guide the EU agents to adjust their day-ahead energy procurement commitments, thereby contributing to the intra-day power balance. After receiving the hourly-ahead price, the EU agents may buy more energy to enhance the comfort level (if the hourly-ahead price gets lower) or sell part of their day-ahead procurement commitments back to the MEMG operator for arbitrage (if the hourly-ahead price gets higher).

Note that the industrial, commercial, and residential agents can reflect three representative load types in real world, which have different preferences on energy demand and comfort requirement, and usually take different responsive strategies to market prices. For instance, the industrial agent may not require a rigorous comfort level but is more sensitive to energy prices. In contrast, the commercial agent may put a priority on the comfort level but has weaker motivation for bill saving from the demand adjustment. The residential agent tends to consider both energy prices and comfort level.

III. Mathematical Modeling

In the MEMG, the operator aims to maximize its operating profit, while the EU agents aim to minimize their individual energy consumption costs. Assuming that the MEMG operator knows the EU agents' preference on energy demand and comfort requirement, it can take the lead in making strategies, hence is a strategy maker. The EU agents can only take strategies to optimize their objectives under the decisions from the MEMG operator, so are strategy takers. Hence, the trading interaction can be modeled by a Stackelberg game [25], in which the MEMG operator acts as a leader and EU agents as three followers. All participants in this game are assumed to be rational, and tend to adjust their strategies until the Stackelberg equilibrium is achieved. Note that the end EUs' preference information is collected and protected by their corresponding EU agents. The MEMG operator just knows the aggregated preference information provided by each EU agent. Only the EU agents know their respective end EUs' information based on contract agreement. Thus, the privacy of the end EUs can be effectively protected.

Generally, a Stackelberg game can be expressed as a bi-level optimization model [15]. For mathematical conciseness, this section firstly formulates the day-ahead joint energy scheduling and trading problem using a deterministic bi-level model. Then the model is extended into a two-stage stochastic model through an adaptive SO approach in Section IV.

A. Deterministic Day-Ahead Bi-Level Model

1) Upper-Level Problem for MEMG Operator: The upper-level problem is to optimize the energy scheduling and pricing strategies for the MEMG operator, aiming to maximize its overall operating profit. The upper-level problem is mathematically expressed as follows.

$$\max \sum_{t \in N_T} \begin{bmatrix} \sum_{i \in N_I} \left(\lambda_{i,t}^{elec} P_{i,t}^{elec} + \lambda_{i,t}^{thm} P_{i,t}^{thm} \right) \\ -\sum_{j \in N_J} \kappa_j^{DG} P_{j,t}^{DG} - \kappa^{BS} (P_t^{BSC} + P_t^{BSD}) \\ -\kappa^{TS} (P_t^{TSC} + P_t^{TSD}) - \kappa^{CCHP} P_t^{CCHP,el} \end{bmatrix} \tag{1}$$

Subject to:

$$\begin{bmatrix} \sum_{j \in N_J} P_{j,t}^{DG} + P_t^{CCHP,el} + P_t^{PV} + P_t^{WT} \\ -P_t^{BSC} + P_t^{BSD} = \sum_{i \in N_I} P_{i,t}^{elec} \end{bmatrix}, \ \forall t \, \epsilon \, N_T \tag{2}$$

$$P_t^{CCHP,th} - P_t^{TSC} + P_t^{TSD} = \sum_{i \in N_I} P_{i,t}^{thm}, \ \forall t \, \epsilon \, N_T \tag{3}$$

$$P_{0,t}^{elec}, P_{0,t}^{thm} \geq 0, \ \forall t \, \epsilon \, N_T \tag{4}$$

$$P_j^{DG,\min} \leq P_{j,t}^{DG} \leq P_j^{DG,\max}, \ \forall t \, \epsilon \, N_T, \ \forall j \in N_J \tag{5}$$

$$R_j^{DG,\min} \leq P_{j,t}^{DG} - P_{j,t-1}^{DG} \leq R_j^{DG,\max}, \ \forall t \, \epsilon \, N_T, \ \forall j \in N_J \tag{6}$$

$$P^{CCHP,\min} \leq P_t^{CCHP,el} \leq P^{CCHP,\max}, \ \forall t \, \epsilon \, N_T \tag{7}$$

$$P_t^{CCHP,th} = \eta^{CCHP} P_t^{CCHP,el}, \ \forall t \in N_T \tag{8}$$

$$0 \le P_t^{BSC} \le P^{BSC,\max}, \ \forall t \in N_T \tag{9}$$

$$0 \le P_t^{BSD} \le P^{BSD,\max}, \ \forall t \in N_T \tag{10}$$

$$P_t^{BSC} P_t^{BSD} = 0, \ \forall t \in N_T \tag{11}$$

$$E_t^{BS} = E_{t-1}^{BS}\left(1-\tau^{BS}\right) + \eta^{BSC} P_t^{BSC} - \frac{P_t^{BSD}}{\eta^{BSD}}, \forall t \in N_T \tag{12}$$

$$\chi_{\min}^{BS} E^{BS,rate} \le E_t^{BS} \le \chi_{\max}^{BS} E^{BS,rate}, \ \forall t \in N_T \tag{13}$$

$$E_0^{BS} = E_{24}^{BS} \tag{14}$$

$$0 \le P_t^{TSC} \le P^{TSC,\max}, \ \forall t \in N_T \tag{15}$$

$$0 \le P_t^{TSD} \le P^{TSD,\max}, \ \forall t \in N_T \tag{16}$$

$$P_t^{TSC} P_t^{TSD} = 0, \ \forall t \in N_T \tag{17}$$

$$E_t^{TS} = E_{t-1}^{TS}\left(1-\tau^{TS}\right) + \eta^{TSC} P_t^{TSD} - \frac{P_t^{TSD}}{\eta^{TSD}}, \ \forall t \in N_T \tag{18}$$

$$\chi_{\min}^{TS} E^{TS,rate} \le E_t^{TS} \le \chi_{\max}^{TS} E^{TS,rate}, \ \forall t \in N_T \tag{19}$$

$$E_0^{TS} = E_{24}^{TS} \tag{20}$$

Objective function (1) is to maximize the overall operating profit of the MEMG operator by energy scheduling and pricing. Therein, the energy trading quantities with the EU agents, i.e., $P_{i,t}^{elec}, P_{i,t}^{thm}$ $(i \in N_I \backslash 0)$, are optimized by the lower-lever EU agents, and thus treated as parameters here. Note that the operator does not buy energy from the exogenous networks, since reselling procured energy cannot make profits in a non-monopoly market. The directions of energy flows trading with the exogenous networks are stated in (4). Eqs. (2)–(3) are the power balance constraints. Eqs. (5)–(6) show the power output bounds and ramping limits for DGs. Eqs. (7)–(8) state the power output limits and energy conversion of the CCHP unit. Eqs. (9)–(14) are the operating constraints for BS and (15)–(20) are for TS.

2) Lower-Level Problems for EU Agents: Each lower-level problem aims to seek the optimal energy procurement strategy for each EU agent $i \in N_I \backslash 0$ based on the energy prices that are determined by the upper-level MEMG operator and treated as parameters at this level. The lower-level problems can be formulated as below, and the corresponding dual variables to each constraint are given after a colon.

$$\left\{ \min \sum_{t \in N_T} \left[\begin{array}{c} \lambda_{i,t}^{elec} P_{i,t}^{elec} + \lambda_{i,t}^{thm} P_{i,t}^{thm} + \\ \lambda_{exo,t}^{elec} P_{i,t}^{el,e} + \lambda_{exo,t}^{thm} P_{i,t}^{th,e} + \\ \alpha_{i,t}\left(P_{i,t}^{ed} - P_{i,t}^{exp}\right)^2 + \beta_{i,t}\left(\theta_{i,t}^{td} - \theta_{i,t}^{exp}\right)^2 \end{array} \right] \right. \tag{21}$$

Subject to:

$$P_{i,t}^{elec} + P_{i,t}^{el,e} = P_{i,t}^{ed} \quad : \nu_{i,t}^{ed}; \ \forall t \in N_T \tag{22}$$

$$P_{i,t}^{thm} + P_{i,t}^{th,e} = P_{i,t}^{td} \quad : \nu_{i,t}^{td}; \ \forall t \in N_T \tag{23}$$

$$P_{i,t}^{elec}, P_{i,t}^{thm} \ge 0 \ : \mu_{i,t}^{elec,m}, \ \mu_{i,t}^{thm,m}; \ \forall t \in N_T \tag{24}$$

$$P_{i,t}^{el,e}, P_{i,t}^{th,e} \ge 0 \ : \ \mu_{i,t}^{elec,e}, \ \mu_{i,t}^{thm,e}; \ \forall t \in N_T \tag{25}$$

$$P_{i,t}^{elec} \le P_i^{elec,\max} \ : \mu_{i,t}^{elec,\max}; \ \forall t \in N_T \tag{26}$$

$$P_{i,t}^{thm} \le P_i^{thm,\max} \ : \mu_{i,t}^{thm,\max}; \ \forall t \in N_T \tag{27}$$

$$P_{i,t}^{ed,\min} \le P_{i,t}^{ed} \le P_{i,t}^{ed,\max} : \ \mu_{i,t}^{ed,\min}, \ \mu_{i,t}^{ed,\max}; \forall t \in N_T \tag{28}$$

$$\sum_{t \in N_T} P_{i,t}^{ed} \ge \gamma_i \sum_{t \in N_T} P_{i,t}^{exp} \ : \ \mu_i^{ed} \tag{29}$$

$$P_{i,t}^{td} = C_i^{air} \ \left(\theta_{i,t-1}^{td} - \theta_{i,t}^{td}\right) + \frac{\left(\theta_{i,t}^{am} - \theta_{i,t}^{td}\right)}{R_i^T} \ : \ \nu_{i,t}^{in}; \forall t \in N_T \tag{30}$$

$$\theta_{i,t}^{td,\min} \le \theta_{i,t}^{td} \le \theta_{i,t}^{td,\max} \ : \ \mu_{i,t}^{td,\min}, \ \mu_{i,t}^{td,\max}; \ \forall t \in N_T \tag{31}$$

$$\left. \right\} \forall i \in N_I \backslash 0$$

Objective function (21) is the utility function of EU agent i, which consists of the energy procurement cost (first four terms) and discomfort cost (last two terms) [4], [26]. Eqs. (22)–(23) state that EU agent i can buy electrical/thermal energy from both the MEMG operator and the exogenous network. Eqs. (24)–(25) restrict the directions of energy trading, considering reselling energy cannot bring any profit for EU agents. Eqs. (26)–(27) are the distribution line/pipe capacity limits. Eqs. (28)–(29) describe the flexibility range of the electrical demand. Assuming the thermal energy is used for district cooling in summer, the temperature-dependent thermal demand is formulated in (30). The heating demand in winter can also be modeled similarly. Eq. (31) means that the indoor temperature can be accepted within a certain range without much loss of comfort.

Note that the different preferences of the EU agents are characterized by different parameter settings in model (21)–(31). The preference on energy demand is specified by $P_{i,t}^{ed,\min}, P_{i,t}^{ed,\max}, \ \theta_{i,t}^{td,\min}, \theta_{i,t}^{td,\max}, \gamma_i$. And the preference on comfort requirement is specified by $\alpha_{i,t}, \beta_{i,t}, P_{i,t}^{exp}, \theta_{i,t}^{exp}$.

B. Single-Level Mathematical Program With Equilibrium Constraints

The upper-level problem is optimized based on the results of the lower-level problems. Thus, the proposed model can be rewritten as the bi-level optimization model below:

$$\max\,(1) \tag{32}$$

$$\text{s.t. } (2)-(20) \tag{33}$$

$$\boldsymbol{P}_i^{elec}, \boldsymbol{P}_i^{thm} \in \text{argmin } (21), \ \forall i \in N_I \backslash 0 \tag{34}$$

$$\text{s.t. } (22)-(31), \ \forall i \in N_I \backslash 0 \tag{35}$$

where $\boldsymbol{P}_i^{elec} := \{P_{i,t}^{elec}\}_{t \in N_T}$ and $\boldsymbol{P}_i^{thm} := \{P_{i,t}^{thm}\}_{t \in N_T}$. The upper-level problem is to optimize the energy scheduling and pricing strategies for the MEMG operator based on the energy procurement strategy of each EU agent. The energy procurement strategies based on specific energy prices are optimized by the lower-level problems.

To solve the bi-level model (32)–(35), one needs to convert it into a single-level model. Since the lower-level models are convex optimization problems with differentiable objective and constraint functions, they can be replaced by their Karush-Kuhn-Tucker (KKT) conditions [27]. The resulting single-level model is given in Appendix A of [37], which is known as a mathematical program with equilibrium constrains (MPEC).

C. Model Linearization

The single-level MPEC model involves three sources of non-linearity. All of them can be linearized below:

1) For the bilinear constraints (11) and (17), they are loose enough and can be removed directly [21]. An alternative way is to use the Big-M approach, which will be specified in 2).
2) For the complementarity conditions in the form of $0 \leq g \perp \mu \geq 0$, the Big-M approach [19] is used to linearize them. The equivalent linearized constraints are $0 \leq g \leq \zeta M$ and $0 \leq \mu \leq (1-\zeta)M$, where ζ is an auxiliary binary variable and M is set to a big positive number.
3) For the bilinear objective function (1), each bilinear term can be linearized by discretizing the energy trading prices, which is inspired by the binary expansion method [28]. Here, the bilinear term $\lambda_{i,t}^{elec} P_{i,t}^{elec}$ $(i \in N_I \backslash 0)$ is taken as an example to illustrate the linearization process as:

S1) Discretize $\lambda_{i,t}^{elec}$ into a sequence of parameters $\varpi_{i,\ t,n}^{elec}$, where n is the index of discretized parameters. Note that pricing strategy has to be subject to a natural interval in the energy market, i.e., $\varpi_{i,\ t,n}^{elec} \in [\lambda_{0,t}^{elec}, \lambda_{exo,t}^{elec}]$.

S2) Express $\lambda_{i,t}^{elec}$ by the following constraints.

$$\lambda_{i,t}^{elec} = \sum_{n \in N} \varphi_{i,t,n}^{elec} \varpi_{i,\ t,n}^{elec},\ \forall t \,\epsilon\, N_T \tag{36}$$

$$\sum_{n \in N} \varphi_{i,t,n}^{elec} = 1,\ \forall t \,\epsilon\, N_T \tag{37}$$

Where $\varphi_{i,t,n}^{elec}$ is an auxiliary binary variable.

S3) Linearize the bilinear term $\lambda_{i,t}^{elec} P_{i,t}^{elec}$ as below.

$$\lambda_{i,t}^{elec}\ P_{i,t}^{elec} = \sum_{n \in N} \varpi_{i,\ t,n}^{elec} P_{i,t,n}^{el},\ \forall t \,\epsilon\, N_T \tag{38}$$

$$0 \leq P_{i,t,n}^{el} \leq \varphi_{i,t,n}^{elec} M,\ \forall n \epsilon N,\ \forall t \,\epsilon\, N_T \tag{39}$$

$$0 \leq \left(P_{i,t}^{elec} - P_{i,t,n}^{el}\right) \leq \left(1 - \varphi_{i,t,n}^{elec}\right) M,\ \forall n \epsilon N, \forall t \,\epsilon\, N_T \tag{40}$$

Where $P_{i,t,n}^{el}$ is an auxiliary continuous variable.

IV. Risk-Averse Adaptive Stochastic Optimization

To coordinate the day-ahead and intra-day stages, this section presents an adaptive (two-stage) SO approach [5], by which the deterministic model in Section III is extended into a day-ahead stochastic model and an intra-day deterministic model. Besides, the risk aversion of the MEMG operator under uncertainties is formulated in the day-ahead stage.

A. Day-Ahead Stochastic Optimization

In the day-ahead optimization, the ambient temperature, the power outputs of PV and WT are modeled as random variables. With their day-ahead probabilistic predictions, Latin hypercube sampling and simultaneous backward reduction are utilized to generate a representative set of scenarios. The detailed scenario generation and reduction procedures can be found in [29].

Given the representative scenario set N_s, the stochastic day-ahead single-level MPEC model can be easily obtained based on the deterministic one in Section III. Considering the page limit, only the compact form is presented as

$$\max\ \boldsymbol{c}^T \boldsymbol{x} + \sum_{s \in N_s} \pi_s \mathcal{L}\left(\boldsymbol{x}, \boldsymbol{d_s}\right) \tag{41}$$

$$\text{s.t. } \boldsymbol{x} \in \boldsymbol{\chi} \tag{42}$$

$$\mathcal{L}\ \left(\boldsymbol{x}, \boldsymbol{d_s}\right) = \max_{\boldsymbol{y}_s \in \Omega(\boldsymbol{x}, \boldsymbol{d_s})} \boldsymbol{b}^T \boldsymbol{y}_s \tag{43}$$

$$\begin{aligned} \text{where}:\ \Omega\ \left(\boldsymbol{x}, \boldsymbol{d_s}\right) \\ = \left\{\boldsymbol{y}_s | \boldsymbol{A}\boldsymbol{x} + \boldsymbol{B}\boldsymbol{y}_s \geq \boldsymbol{r},\ \boldsymbol{E}\boldsymbol{x} + \boldsymbol{F}\ \boldsymbol{y}_s = \boldsymbol{d_s}\right\} \end{aligned} \tag{44}$$

The adaptive SO approach classifies the variables into two groups. $\boldsymbol{x}$ represents the first-stage variables, including the scheduling decisions on DGs and ESSs as well as the day-ahead energy trading prices. $\boldsymbol{y}_s$ denotes the second-stage variables which include all remaining primal and dual variables. Objective (41) is to find a day-ahead solution $\boldsymbol{x}^*$ to maximize the expectation over all representative scenarios, where π_s is the probability of scenario s. In (42), $\boldsymbol{\chi}$ gives the feasible region of the first-stage variables $\boldsymbol{x}$. Eqs. (43)–(44) state that $\boldsymbol{y}_s$ is optimized under $\boldsymbol{x}$ and individual uncertainty scenarios $\boldsymbol{d_s}$.

B. Uncertainty Risk Minimization

The day-ahead optimization stated in (41)–(44) can derive an optimal solution $\boldsymbol{x}^*$, which is solved by maximizing the expectation over all representative scenarios. This means $\boldsymbol{x}^*$ may be optimistic and result in a disappointing profit under some unfavorable scenarios. However, a risk-averse MEMG operator does not want to suffer a large deviation from the expected profit. To consider the risk aversion of the MEMG operator towards uncertainties, a CVaR measure [5] is applied in this paper, which is formulated as

$$CVaR_\vartheta = \min_{\eta \epsilon \mathcal{R}} \left\{\eta + \frac{1}{1-\vartheta} \sum_{s \in N_s} \left[f_L^s - \eta\right]^+ \pi_s\right\} \tag{45}$$

where η is an auxiliary variable called value-at-risk (VaR); f_L^s is the loss function; $[\cdot]^+$ denotes a projection operator, i.e., $[\aleph]^+ = \max(\aleph, 0)$. $\sum_{s \in N_s} \left[f_L^s - \eta\right]^+ \pi_s$ gives the expected risk above a specific VaR. ϑ is the confidence level.

The uncertainty risk for the MEMG operator in this paper refers to the risk of the low profit in some unfavorable scenarios.

Therefore, $CVaR_\vartheta$ is rewritten in the form of "*max*" as:

$$CVaR_\vartheta = \max_{\eta\epsilon\mathcal{R}} \left\{ \eta + \frac{1}{1-\vartheta} \sum_{s\in N_s} [f_P^s - \eta]^- \pi_s \right\} \quad (46)$$

where $f_P^s = \boldsymbol{c}^T\, \boldsymbol{x} + \mathcal{L}(\boldsymbol{x}, \boldsymbol{d_s})$ denotes the profit under scenario s. $[\cdot]^-$ denotes the projector of $\min(\cdot, 0)$.

For risk aversion, the objective function in the day-ahead optimization is modified as below.

$$\max_{\boldsymbol{x}\in\boldsymbol{\chi},\ \boldsymbol{y}_s\in\Omega,\ \eta\epsilon\mathcal{R}} \boldsymbol{c}^T\boldsymbol{x} + \sum_{s\in N_s} \pi_s \mathcal{L}\left(\boldsymbol{x}, \boldsymbol{d_s}\right) + \rho\cdot CVaR_\vartheta \quad (47)$$

where ρ is the weighting factor of CVaR.

The newly introduced nonlinear term $[f_P^s - \eta]^-$ can be replaced by $\Re_s$. $\Re_s$ is subject to two linear inequalities:

$$\Re_s \leq 0,\ \Re_s \leq f_P^s - \eta \quad (48)$$

where $\Re_s$ is an auxiliary variable.

C. Intra-Day Deterministic Optimization

In the intra-day optimization, the values of uncertain parameters are updated by their hourly-ahead point predictions, but the day-ahead schedules on electrical/thermal storage and DGs remain unchanged in this stage. To address the intra-day (hourly-ahead) power imbalance, this stage aims to reschedule the CCHP unit hourly, while determining the hourly-ahead trading prices in the intra-day market to guide the EU agents to adjust their day-ahead energy procurement commitments by intra-day energy trading. Note that the intra-day energy trading strategies of the MEMG operator and EU agents should be made based on their day-ahead trading commitments. For instance, the quantities that the EU agents sell in the intra-day market cannot be larger than their day-ahead energy procurement commitments.

The objectives of the intra-day upper- and lower-level problems are formulated as:

- **Intra-day objective function for the MEMG operator**

$$\begin{aligned}\Bigg\{ &\max \sum_{i\in N_I\backslash 0} \left(\Lambda_{i,t}^{elec}\Delta P_{i,t}^{elec} + \Lambda_{i,t}^{thm}\Delta P_{i,t}^{thm}\right) \\ &- \kappa^{CCHP} P_t^{CCHP,el} + \Lambda_{0,t}^{elec}\left[\Delta P_{0,t}^{elec}\right]^+ \\ &+ \Lambda_{exo,t}^{elec}\left[\Delta P_{0,t}^{elec}\right]^- + \Lambda_{0,t}^{thm}\left[\Delta P_{0,t}^{thm}\right]^+ \\ &+ \Lambda_{exo,t}^{thm}\left[\Delta P_{0,t}^{thm}\right]^- \Bigg\}\ \forall t\,\epsilon\, N_T \end{aligned} \quad (49)$$

- **Intra-day objective function for each EU agent**

$$\begin{aligned}\Big\{ &\min\ \Lambda_{i,t}^{elec}\Delta P_{i,t}^{elec} + \Lambda_{i,t}^{thm}\Delta P_{i,t}^{thm} \\ &+ \alpha_{i,t}\left(P_{i,t}^{ed} - P_{i,t}^{exp}\right)^2 \\ &+ \beta_{i,t}\left(\theta_{i,t}^{td} - \theta_{i,t}^{exp}\right)^2 + \Lambda_{exo,t}^{elec}\left[\Delta P_{i,t}^{el,e}\right]^+ + \Lambda_{0,t}^{elec}\left[\Delta P_{i,t}^{el,e}\right]^- \\ &+ \Lambda_{exo,t}^{thm}\left[\Delta P_{i,t}^{th,e}\right]^+ \\ &+ \Lambda_{0,t}^{thm}\left[\Delta P_{i,t}^{th,e}\right]^- \Big\}\ \forall i \in N_I\backslash 0,\ \forall t\,\epsilon\, N_T \end{aligned} \quad (50)$$

Considering the intra-day bi-level model has a similar formulation to the day-ahead one in Section III. Its constraints can be obtained simply by the following two steps:

1) For constraints in bi-level model (32)–(35), replace $P_{i,t}^{elec/thm}$ by $P_{i,t}^{elec/thm*} + \Delta P_{i,t}^{elec/thm}$ and $P_{i,t}^{el/th,e}$ by $P_{i,t}^{el/th,e*} + \Delta P_{i,t}^{el/th,e}$, where $P_{i,t}^{elec/thm*}$, $P_{i,t}^{el/th,e*}$ are the energy trading commitments of the operator and EU agents made in the day-ahead market.
2) Decouple (29) into single-period constraints as $P_{i,t}^{ed} \geq \Gamma_i P_{i,t}^{ed,fir*}$, where $\Gamma_i = \gamma_i \sum_{t\in N_T} P_{i,t}^{exp} / \sum_{t\in N_T} P_{i,t}^{ed,fir*}$ and $P_{i,t}^{ed,fir*}$ is the day-ahead electrical procurement of EU agent *i*.

Generally, $\Lambda_{exo,t}^{elec/thm}$ is higher than $\Lambda_{0,t}^{elec/thm}$. Hence, the operator $[\cdot]^{+/-}$ in the intra-day objectives can be easily removed by introducing two non-negative auxiliary variables. For example, let $\Delta P_{i,t}^{el/th,e} = B_{i,t}^{el/th,e} - S_{i,t}^{el/th,e}$, where $B_{i,t}^{el/th,e}$, $S_{i,t}^{el/th,e} \geq 0$. Then $[\Delta P_{i,t}^{el/th,e}]^+$ and $[\Delta P_{i,t}^{el/th,e}]^-$ can be replaced directly by $B_{i,t}^{el/th,e}$ and -$S_{i,t}^{el/th,e}$.

The complete intra-day bi-level model is given in Appendix B, and its single-level MPEC is presented in Appendix C of [37].

D. Flowchart of Proposed Transactive Energy Management

The implementation of the proposed transactive energy management method is shown in the flowchart as Fig. 2.

In the day-ahead energy market, the first step is to formulate the day-ahead upper-level model for the MEMG operator and the day-ahead lower-level models for the individual EU agents, as presented in Section III-A. The MEMG operator as a price maker aims to set the day-ahead prices to each EU agent. Then, the EU agents as price takers respond to the received prices by determining their energy trading quantities. To obtain the market equilibrium while considering the underlying impacts of uncertainties as well as the MEMG operator's risk aversion towards uncertainties, a day-ahead stochastic single-level MPEC model with a CVaR measure is then formulated using the day-ahead probabilistic predictions of uncertainties as inputs. The day-ahead stochastic model is solved by an adaptive PH algorithm, which will be introduced in Section V-A.

In the intra-day energy market, the strategies are made based on the day-ahead energy scheduling decisions on ESSs and DGs as well as the day-ahead energy trading commitments. Similarly, the intra-day upper-level and lower-level models are firstly formulated, which are coupled by the intra-day energy trading prices and quantities. Then in order to seek the intra-day market equilibrium, the intra-day bi-level model is reformulated as an intra-day deterministic single-level MPEC model, which is later solved by an OA algorithm as stated in following Section V-B.

V. Solution Methods

For high-performance solution, this section proposes two iterative algorithms for solving the day-ahead and intra-day

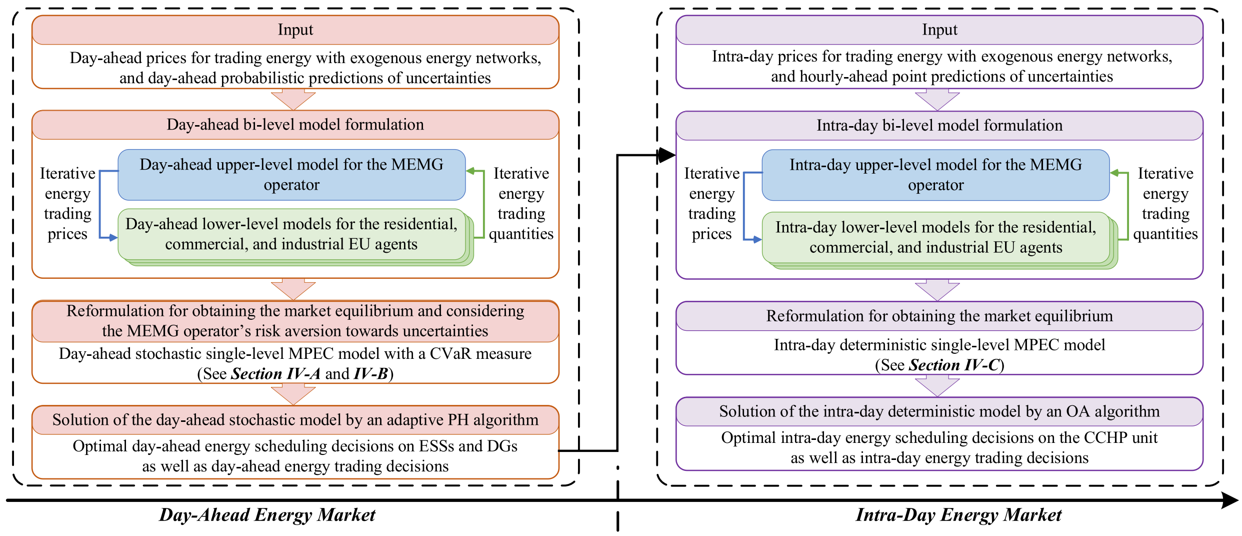

Fig. 2. Flowchart of the proposed transactive energy management.

optimization, respectively. An adaptive Progressive Hedging (PH) algorithm is developed to seek the day-ahead near-optimal solution in an effective and timely manner, which decomposes the day-ahead stochastic MILP problem into scenario-based subproblems and solves these subproblems in parallel. In the intra-day stage, an outer approximation (OA) algorithm is adopted to solve the bilinear problem without the introduction of binary variables.

A. Adaptive PH Algorithm for Day-Ahead Stochastic MILP

In the literature, most of the works use commercial solvers, e.g., GUROBI, to directly solve stochastic problems. However, solving a stochastic MIP may be computationally difficult for existing solvers, especially when the MIP model has a large number of integer variables. Therefore, many decomposition algorithms have been proposed for improving computational efficiency. Two dominant classes are stage-based algorithms (e.g., L-shaped method [30] and Benders decomposition [31]) and scenario-based algorithms (e.g., dual decomposition [32] and Progressive Hedging algorithm [33]). Compared with the stage-based decomposition, the scenario-based decomposition can achieve a more uniform distribution of computation load to each subproblem, which is beneficial to parallel computing. Besides, L-shaped and Benders methods are restricted when the second-stage problem is non-convex with integer variables [34]. In contrast, PH algorithm imposes fewer restrictions on stochastic MIP. Moreover, it generally converges faster than dual decomposition method [35]. PH algorithm decomposes a stochastic MIP into multiple scenario-based subproblems, and can solve them in parallel to obtain a convergent near-optimal solution. However, the PH algorithm in [33] cannot balance the solution accuracy and convergence speed. Thus, in order for a better computation performance, an adaptive PH algorithm is further developed by adopting an adjustable penalty factor to achieve a high computation efficiency, while guaranteeing an acceptable solution quality.

To demonstrate the adaptive PH algorithm, the day-ahead stochastic MILP is expressed in a compact form as:

$$\begin{aligned}
&\max\ \boldsymbol{c}^T\boldsymbol{x} + \sum_{s\in N_s}\pi_s\boldsymbol{b}^T\boldsymbol{y}_s + \rho\cdot\left(\eta + \frac{1}{1-\vartheta}\sum_{s\in N_s}\pi_s\Re_s\right)\\
&\quad = \boldsymbol{c}^T\boldsymbol{x} + \rho\eta + \sum_{s\in N_s}\pi_s\left(\boldsymbol{b}^T\boldsymbol{y}_s + \frac{\Re_s}{1-\vartheta}\right)\\
&\quad = \mathcal{C}^T\,\mathcal{x} + \sum_{s\in N_s}\pi_s\mathcal{B}^T\mathcal{y}_s \qquad (51)
\end{aligned}$$

$$\text{s.t. } (\mathcal{x}, \mathcal{y}_s) \in \mathcal{Q}_s, \forall s \in N_s \qquad (52)$$

where $\mathcal{x} := \{\boldsymbol{x},\ \eta\}$ denotes the first-stage variables and $\mathcal{y}_s := \{\boldsymbol{y}_s, \Re_s\}$ represents the second-stage variables. $\mathcal{C}$ and $\mathcal{B}$ are the augmented coefficient vectors associated with $\mathcal{x}$ and $\mathcal{y}_s$. Eq. (52) gives the constraints under each scenario.

The proposed adaptive PH algorithm for solving the day-ahead stochastic MILP model (51)–(52) is described in Algorithm 1.

The adaptive PH algorithm starts by solving the subproblems under each scenario and calculating the expected value $\overline{\mathcal{x}}$ and multiplier $\boldsymbol{\eta}_s$ with an initial penalty factor $\mathcal{P}$. Step 7 adjusts the discrete distribution of energy trading prices to reduce the number of integer variables. After the initialization phase (Step 1-7), the augmented subproblems are solved in Step 11 and $\overline{\mathcal{x}}$, $\boldsymbol{\eta}_s$ are updated in Step 15-16. The iterative phase terminates until the stop criteria is satisfied in Step 18, i.e., all first-stage decisions $\mathcal{x}_s$ converge to $\overline{\mathcal{x}}$. Notice that when $\tau \geq \tau_1$, a bigger penalty factor $\mathcal{P}_1$ can be used to accelerate the convergence process, but the initial penalty factor $\mathcal{P}$ should be set as a small value for high solution accuracy.

B. OA Algorithm for Intra-Day Bilinear Problem

A linearization method for addressing the bilinear terms of the objective function has been introduced in Section III-C. For

Algorithm 1: The Adaptive PH Algorithm.

Initialize the iteration index τ=0. Set an initial penalty factor $\mathcal{P}$ and a tolerance level ε.
for s=1 **to** N_s **do**
  $\boldsymbol{x}_s^{(\tau)} := \operatorname{argmax}_{\boldsymbol{x}} \{\boldsymbol{\mathcal{C}}^T\boldsymbol{x} + \boldsymbol{\mathcal{B}}^T\boldsymbol{y}_s : (\boldsymbol{x}, \boldsymbol{y}_s) \in \boldsymbol{Q}_s\}$
  $\overline{\boldsymbol{x}}^{(\tau)} := \sum_{s\in N_s} \pi_s \boldsymbol{x}_s^{(\tau)}$
  $\boldsymbol{\eta}_s^{(\tau)} := \mathcal{P}(\boldsymbol{x}_s^{(\tau)} - \overline{\boldsymbol{x}}^{(\tau)})$
end
Adjust the discretized values of trading prices according to the results under each scenario in the initialization phase.
repeat
  $\tau = \tau + 1$
  for s=1 **to** N_s **do**
    $\boldsymbol{x}_s^{(\tau)} := \operatorname{argmax}_{\boldsymbol{x}} \{\boldsymbol{\mathcal{C}}^T\boldsymbol{x} + \boldsymbol{\mathcal{B}}^T\boldsymbol{y}_s - \boldsymbol{\eta}_s^{(\tau-1)}\boldsymbol{x} - \frac{\mathcal{P}}{2}||\boldsymbol{x} - \overline{\boldsymbol{x}}^{(\tau-1)}||^2 : (\boldsymbol{x}, \boldsymbol{y}_s) \in \boldsymbol{Q}_s\}$
    if $\tau \geq \tau_1$ **then**
      Adjust the penalty factor, i.e., let $\mathcal{P} = \mathcal{P}_1$
    end if
    $\overline{\boldsymbol{x}}^{(\tau)} := \sum_{s\in N_s} \pi_s \boldsymbol{x}_s^{(\tau)}$
    $\boldsymbol{\eta}_s^{(\tau)} := \boldsymbol{\eta}_s^{(\tau-1)} + \mathcal{P}(\boldsymbol{x}_s^{(\tau)} - \overline{\boldsymbol{x}}^{(\tau)})$
  end
until $\sum_{s\in N_s} \pi_s ||\boldsymbol{x}_s^{(\tau)} - \overline{\boldsymbol{x}}^{(\tau)}|| < \varepsilon$

TABLE II
TECHNICAL PARAMETERS FOR GENERATORS OF MEMG [21]

Units	P^{min}(MW)	P^{max}(MW)	$\kappa^{DG/CCHP}$(\$/MWh)
DG 1-3	(0.45, 0.3, 0.3)	(1.5, 1.0, 1.0)	(122, 134, 136)
CCHP	0	1.5	159

the sake of discussion, the above method is named as the price discretizing method in this paper. The price discretizing method can remove bilinear terms and export a linear objective function. However, it introduces a large number of 0-1 binary variables which increases the computation burden significantly. Hence, an OA algorithm is utilized to solve the intra-day bilinear problem. OA algorithm is an iterative algorithm, which first linearizes the bilinear terms in the objective function around intermediate solution points and then add the derived linear approximations to the OA formulation [36]. Compared with the price discretizing method, OA algorithm can not only improve the computation efficiency by avoiding the introduction of binary variables, but also generate continuous price signals for achieving more accurate demand response control.

Due to the page limit, the detailed procedure of OA algorithm for solving the intra-day bilinear optimization problem is described in Appendix D of [37].

VI. CASE STUDY

A. Testing System

The time horizon of the day-ahead optimization is set to 24 hours with one-hour interval. The stochastic scenarios are generated according to different prediction accuracy. The maximum prediction errors are set as 30% of their forecasts for the renewable generation and 5% for the ambient temperature, as shown in Fig. 3. The intra-day optimization of MEMG is implemented hourly with the hourly-ahead point predictions. Tables II and III show the technical parameters for the generators

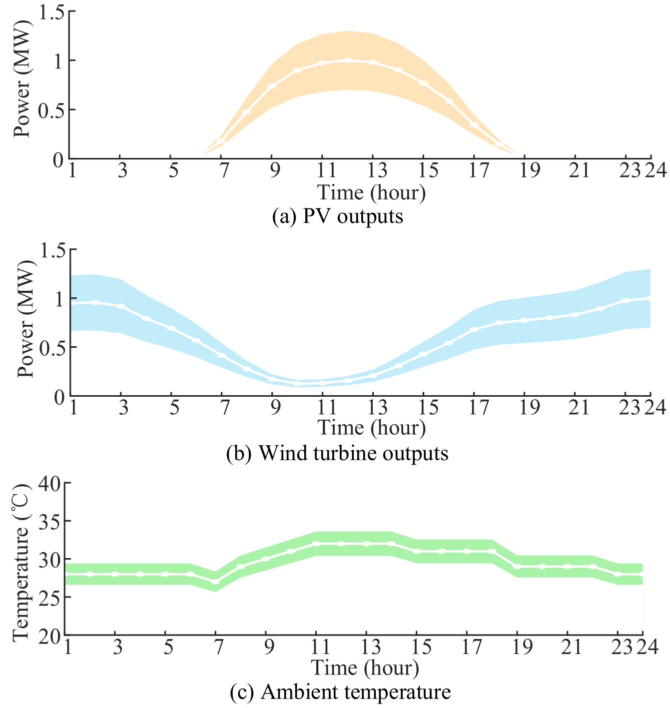

Fig. 3. Day-ahead predictions of renewable generation and ambient temperature.

TABLE III
TECHNICAL PARAMETERS FOR ENERGY STORAGE OF MEMG [21]

Storage	$\chi_{min}^{B/TS}$/ $\chi_{max}^{B/TS}$	$\eta^{B/TSC}$/ $\eta^{B/TSD}$	$\tau^{B/TS}$	$E^{B/TS,rate}$ (MW)	$\kappa^{B/TS}$ (\$/MWh)
BS	0.2/0.9	0.98/0.98	0.01	2.0	30
TS	0.1/0.9	0.95/0.95	0.04	2.5	0.2

TABLE IV
PARAMETERS FOR THREE TYPES OF EUS

EU Type	Residential EUs	Commercial EUs	Industrial EUs
α(\$/MW^2)	826	900	600
β(\$/°C^2)	0.366	0.6 (7:00-20:00) 0 (other periods)	0
γ	0.7	0	1
θ^{exp}(°C)	20	20	N/A
$\theta^{td,min/max}$(°C)	17/25	18/23	N/A
C^{air}(MW/°C)	0.106	0.037	N/A
R^T(°C/MW)	14	65	N/A

and energy storage, respectively. Table IV gives the parameters associated with the residential, commercial and industrial EUs. The selling/buying prices for trading energy with the exogenous energy networks can be found in Fig. 4(c) and the expected energy demand of each EU agent can be found in Fig. 5. In terms of risk aversion modelling, the confidential level ϑ is set as 0.9 and CVaR weight factor ρ is 0.1 [5]. In the adaptive PH algorithm, the tolerance ε and the value of τ_1 are set to 10^{-4} and 15, respectively. The tolerance δ in OA algorithm is set to 10^{-5}.

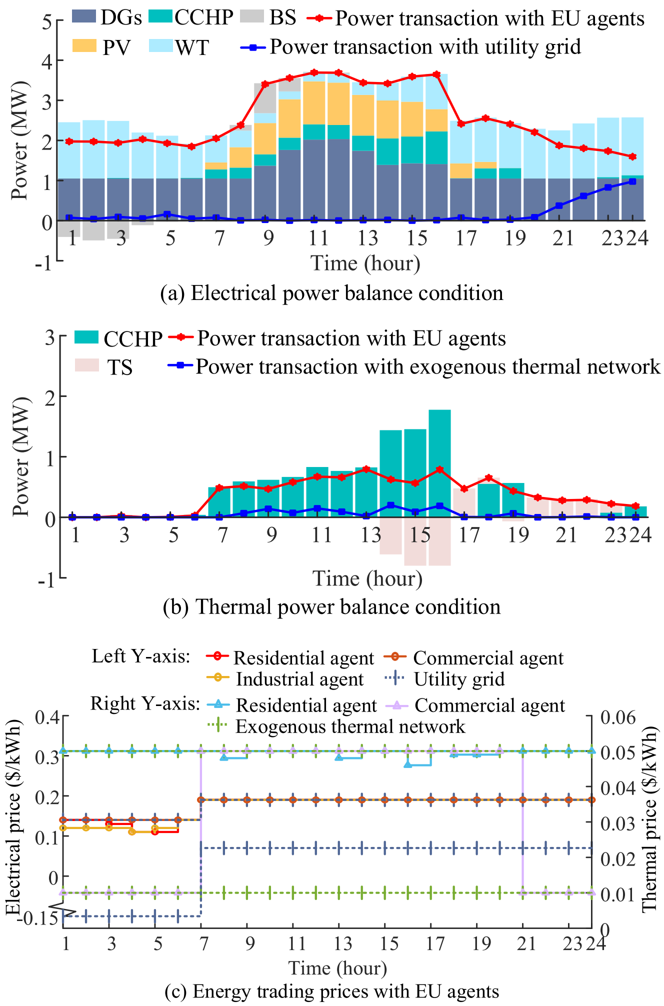

Fig. 4. Day-ahead energy scheduling and pricing decisions of MEMG operator.

All tests in this section are implemented on an Intel(R) Xeon(R) E5-1630 3.70 GHz 64-bit PC with 16GB RAM and solved by GUROBI on MATLAB.

B. Day-Ahead Optimization Results

With the day-ahead probabilistic predictions, 2000 scenarios are initially generated by Latin hypercube sampling method and then reduced to five representative scenarios via simultaneous backward reduction. The day-ahead results are illustrated from the perspectives of the MEMG operator, EU agents and computational performance.

1) From the Perspective of the MEMG Operator: Fig. 4 shows the day-ahead energy scheduling and pricing strategies of the MEMG operator. From the energy scheduling decisions [Fig. 4(a), (b)], it can be seen that the operator mainly transacts with the EU agents, and only a small part of energy is exported to the exogenous networks, as shown by the red and blue lines. It is also worth noting that the CCHP unit does not output any thermal energy during the off-peak period (1:00–6:00) as shown in Fig. 4(b). This is because both the MEMG and utility grid are in a state of over generation, such that the surplus electricity has to be accommodated at a negative feed-in tariff. Hence, the MEMG operator minimizes the power output of the CCHP unit during 1:00–6:00. From the energy pricing decisions [Fig. 4(c)], we can see that the electrical and thermal prices for transacting with the commercial agent (i.e., the reddish brown and purple lines) are equal to the prices for buying energy from the exogenous energy networks. This is because the commercial EU agent has higher requirement for comfort level, thus is not sensitive to the prices released by the MEMG operator. The electrical prices for the residential and industrial agents (i.e., the red and yellow lines) are lower than the selling price of utility grid during the off-peak period (1:00–6:00), since the negative feed-in tariffs compel the operator to stimulate the price-sensitive EUs to accommodate the surplus electrical generation. The thermal prices for the residential agent (i.e., the light blue line) are slightly lower than the selling prices of the exogenous thermal network only at a few time slots. It can be concluded that the day-ahead energy management of the MEMG operator mainly relies on energy scheduling, and pricing strategy acts as a secondary means.

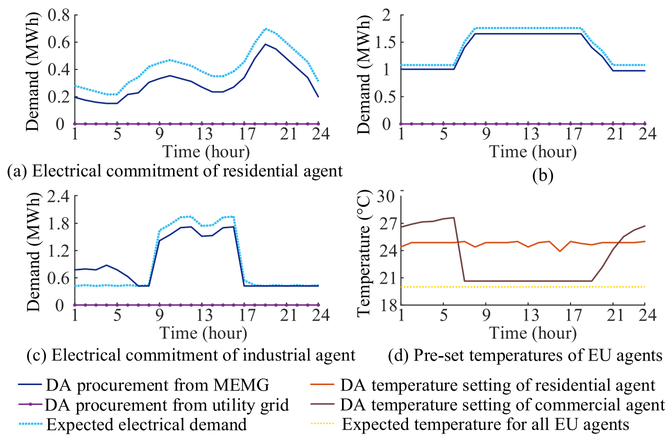

Fig. 5. Day-ahead energy procurement commitments of EU agents.

2) From the Perspective of the EU Agents: The day-ahead (DA) energy procurement commitments of the different EU agents are depicted in Fig. 5. Fig. 5(a) and (b) shows that both the residential and commercial agents procure less electricity than their expected demands in the day-ahead market, which suggests their electrical demands tend to be power-shiftable. In addition, the day-ahead electrical energy procurement commitment of the commercial agent is very close to its expected demand since the commercial EUs are not sensitive to prices. In contrast, Fig. 5(c) shows that the price-sensitive industrial agent shifts a part of electrical energy demand from the peak period (9:00–17:00) to off-peak period (1:00–6:00) and the total daily demand is almost unchanged. This suggests the electrical demand of the price-sensitive industrial agent tends to be time-shiftable. Fig. 5(d) shows the commercial agent has higher comfort requirement on indoor temperature than the residential agent during the working period (7:00–20:00). When the thermal price released by the MEMG operator is reduced [Fig. 4(c)], the relatively sensitive residential agent tends to buy more cooling energy to make the indoor temperature closer to the expected one, as shown by the orange line in Fig. 5(d).

TABLE V
COMPUTATIONAL PERFORMANCE FOR SOLVING THE DAY-AHEAD STOCHASTIC MILP

Solution Approach	No. of Variables	Solution Time	Objective Value ($)	Optimality Accuracy
Direct Use of GUROBI	14862 continuous 4641 binary for all scenarios	79.70 Hours	7501.01	100%
PH Algorithm 1	3938 continuous 2781 binary for each scenario	≥3.21 Hours	N/A	N/A
PH Algorithm 2		0.56 Hours	7478.15	99.7%
Adaptive PH Algorithm		0.71 Hours	7492.69	99.9%

3) Computational Performance: The comparison of the computational performances using an off-the-shelf solver (GUROBI), PH algorithm and adaptive PH algorithm is shown in Table V. The general method is to employ GUROBI to directly solve the day-ahead stochastic MILP for a 100% optimal solution, but it is time-consuming due to the huge number of variables, especially binary variables. In contrast, PH algorithm can effectively reduce the scale of the stochastic MILP problem by scenario decomposition and allow each scenario-based sub-problem to be solved in parallel. To ensure the accuracy of the near-optimal solution, PH algorithm 1 sets $\mathcal{P} = \mathcal{P}_1 = 100$, but it cannot converge within 1000 iterations (3.21 hours). PH algorithm 2 sets $\mathcal{P} = \mathcal{P}_1 = 1000$, the near-optimal solution can be obtained within 0.56 hours, but the accuracy is only 99.7%. To achieve a fast convergence speed while guaranteeing an acceptable solution quality, the proposed adaptive PH algorithm adopts a time-varying penalty factor, i.e., $\mathcal{P} = 100, \mathcal{P}_1 = 1000$. By doing so, a near-optimal solution with 99.9% accuracy can be obtained within 0.71 hours, which is fully compatible with the day-ahead computation. Note that the solution time associated with the (adaptive) PH algorithm is parallel computation time.

C. Intra-Day Optimization Results

The energy trading decisions of the MEMG operator and EU agents in the intra-day (ID) energy market are shown in Fig. 6. For illustration purpose, the day-ahead (DA) energy trading prices are also presented, which are shown by the blue lines in Fig. 6(a)–(c) and the orange lines in Fig. 6(d)–(e).

From the ID electrical energy trading results [Fig. 6(a)–(c)], it can be observed that when the ID electrical price (i.e., the gray line) becomes lower than the DA one, the EU agents tend to buy some additional electricity in the intra-day market to raise their comfort level. In contrast, when the ID price gets higher, the EU agents tend to sell part of their DA procurement back to the MEMG operator for arbitrage. The observation does not fully hold in Fig. 6(c), since the industrial agent cannot lower its DA procurement in the intra-day stage for ensuring the required daily demand, even when the ID price gets higher.

From the ID thermal energy trading results [Fig. 6(d), (e)], it can be found that the EU agents still sell part of their DA thermal procurement at some time slots when the ID price (i.e., the dark brown line) gets lower than the DA one. This behavior is caused by the hourly-ahead ambient temperature reduction compared to the DA prediction, which decreases the ID thermal demands of the EU agents.

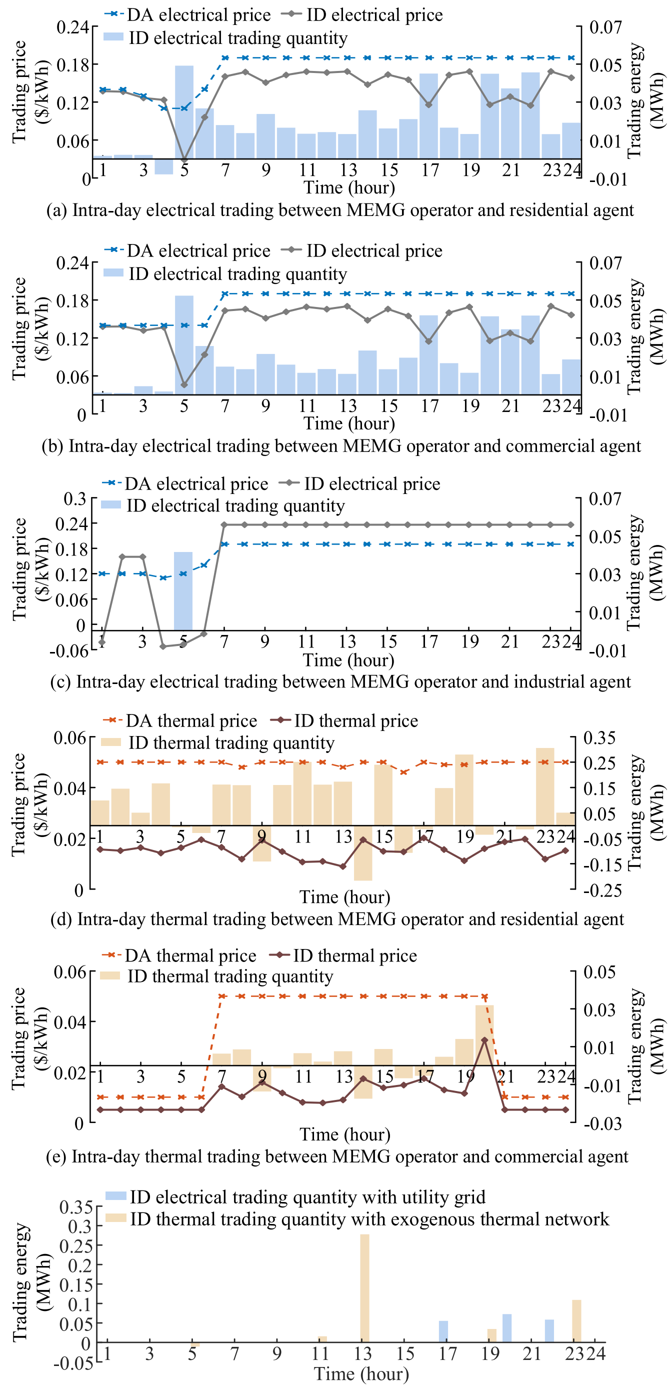

(a) Intra-day electrical trading between MEMG operator and residential agent
(b) Intra-day electrical trading between MEMG operator and commercial agent
(c) Intra-day electrical trading between MEMG operator and industrial agent
(d) Intra-day thermal trading between MEMG operator and residential agent
(e) Intra-day thermal trading between MEMG operator and commercial agent
(f) Intra-day energy trading between MEMG operator and exogenous networks

Fig. 6. Intra-day energy trading prices and quantities.

Fig. 6(f) shows the MEMG operator exchanges electrical/thermal energy with the exogenous energy networks in the ID energy market only at a few time slots. This means, the ID local power balance can be achieved by the pricing strategy of the MEMG operator at most of time. Hence, it can be concluded that the intra-day transactive energy management can effectively reduce the MEMG's reliance on the exogenous energy networks.

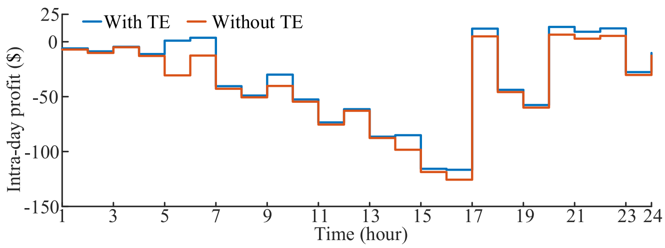

Fig. 7. Intra-day profit of MEMG operator.

TABLE VI
COMPUTATION TIME FOR THE INTRA-DAY OPTIMIZATION

Bilinear Term Linearization Approach	Step Size ($/kWh)	Convergence Tolerance	Average Time (s)
Price Discretizing	0.001	N/A	191.95
OA Algorithm	→ 0	10^{-5}	13.51

The intra-day operating profits of the MEMG operator with and without considering transactive energy (TE) are shown in Fig. 7. Note that the intra-day operating profits here do not include the day-ahead determined profits (i.e., the sales revenue in the day-ahead market minus the operating costs of DGs and ESSs). The lower operating profit means the MEMG operator spends more cost on addressing the intra-day power imbalance caused by the uncertain renewable generation. Fig. 7 illustrates that without the intra-MEMG TE, the MEMG operator has to cost more to balance the intra-day power deviation since it can only reschedule the CCHP unit and transact with the exogenous energy networks at unfavorable prices. In contrast, with TE, the MEMG operator can guide the EU agents to adjust their day-ahead energy procurement commitments and participate in the demand-side management by releasing proper prices that are beneficial to both sides. Hence, with TE, the MEMG operator can not only reduce the cost spent on addressing intra-day power imbalance [Fig. 7], but also reduce the MEMG's reliance on the exogenous energy networks [Fig. 6(f)].

Table VI compares the computation efficiency using the price discretizing method and OA algorithm for solving the intra-day bilinear problem. It can be observed that the OA algorithm can derive the continuous trading prices (i.e., step size $\rightarrow 0$), while achieving a much faster solution speed.

VII. CONCLUSION

In this paper, a transactive energy management method is proposed for a MEMG. The problem is formulated as a Stackelberg game-based bi-level model that can effectively capture the strategic interactions between the MEMG operator and industrial, commercial, residential agents. To coordinate their strategies in the day-ahead and intra-day energy markets, an adaptive SO approach is presented, while a CVaR measure is used to model the risk aversion of the MEMG operator toward uncertainties in the day-ahead stage. For high-efficiency computation performance, an adaptive PH algorithm is developed to decompose the day-ahead stochastic MILP into scenario-based subproblems that can be solved in parallel. An OA algorithm is adopted to solve the intra-day bilinear problem in a faster way by avoiding the introduction of binary variables.

The simulation results demonstrate that: 1) The proposed transactive energy management method can simultaneously provide optimal energy scheduling and pricing strategies for the MEMG operator, by which the demand-side management can be effectively utilized; 2) The transactive energy management can guide the EU agents to adjust their day-ahead commitments by releasing proper prices that are beneficial to both sides, by which the MEMG's reliance on the exogenous networks can be effectively reduced; 3) The adaptive PH algorithm and OA algorithm can effectively address the multi-scenario stochastic MILP and the bilinear problems, respectively. They both can achieve the significant improvement in computation efficiency. Thus, the effectiveness of the proposed transactive energy management method as well as the efficiency of the adaptive PH and OA algorithms are corroborated.

In this work, only a single MEMG operator and three representative EU agents are involved in the local energy markets, which aims to provide a timely reference for the transactive energy management of MEMGs. In the future work, efforts will be made for the extension of market participants, where a multi-leader multi-follower Stackelberg game can be considered to capture the interactions between multiple energy producers and consumers. Moreover, multi-energy network operation models can be formulated for guaranteeing network-constraint-feasible energy trading actions. Last but not the least, distributed algorithms can be developed to share the computational burden among all market participants, thereby achieving enhanced scalability.

REFERENCES

[1] E. Guelpa, A. Bischi, V. Verda, M. Chertkov, and H. Lund, "Towards future infrastructures for sustainable multi-energy systems: A review," *Energy*, vol. 184, pp. 2–21, 2019.

[2] P. Mancarella, "MES (multi-energy systems): An overview of concepts and evaluation models," *Energy*, vol. 65, pp. 1–17, 2014.

[3] Y. Chen, X. Feng, Z. Li, Y. Xu, and A. Miragha, "Multi-stage coordinated operation of a multi-energy microgrid with residential demand response under diverse uncertainties," *Energy Convers. Econ.*, vol. 1, no. 1, pp. 20–33, 2020.

[4] S. Sharma, A. Verma, Y. Xu, and B. K. Panigrahi, "Robustly coordinated bi-level energy management of a multi-energy building under multiple uncertainties," *IEEE Trans. Sustain. Energy*, vol. 12, no. 1, pp. 3–13, Jan. 2021, doi: 10.1109/tste.2019.2962826.

[5] Z. Li, L. Wu, and Y. Xu, "Risk averse coordinated operation of a multi energy microgrid considering voltage/var control and thermal flow: An adaptive stochastic approach," *IEEE Trans. Smart Grid*, vol. 12, no. 5, pp. 3914–3927, Sep. 2021.

[6] T. G. A. C. (GWAC), "Gridwise transactive energy framework," Pacific Northwest National Lab.(PNNL), Richland, WA, USA, Tech. Rep. PNNL-22946, 2015.

[7] L. P. M. I. Sampath, A. Paudel, H. D. Nguyen, E. Y. Foo, and H. B. Gooi, "Peer-to-peer energy trading enabled optimal decentralized operation of smart distribution grids," *IEEE Trans. Smart Grid*, vol. 13, no. 1, pp. 654–666, Jan. 2022.

[8] K. Zhang, B. Zhou, C. Y. Chung, S. Bu, Q. Wang, and N. Voropai, "A coordinated multi-energy trading framework for strategic hydrogen provider in electricity and hydrogen markets," *IEEE Trans. Smart Grid*, to be published, doi: 10.1109/TSG.2022.3154611.

[9] F. Lezama, J. Soares, P. Hernandez-Leal, M. Kaisers, T. Pinto, and Z. Vale, "Local energy markets: Paving the path toward fully transactive energy systems," *IEEE Trans. Power Syst.*, vol. 34, no. 5, pp. 4081–4088, Sep. 2019, doi: 10.1109/tpwrs.2018.2833959.

[10] X. Jiang, C. Sun, L. Cao, L. Ngai-Fong, and K. H. Loo, "Peer-to-peer energy trading with energy path conflict management in energy local area network," *IEEE Trans. Smart Grid*, vol. 13, no. 3, pp. 2269–2278, May 2022, doi: 10.1109/TSG.2022.3141236.
[11] Z. Yang, J. Hu, X. Ai, J. Wu, and G. Yang, "Transactive energy supported economic operation for multi-energy complementary microgrids," *IEEE Trans. Smart Grid*, vol. 12, no. 1, pp. 4–17, Jan. 2021, doi: 10.1109/tsg.2020.3009670.
[12] J. Li, M. E. Khodayar, J. Wang, and B. Zhou, "Data-driven distributionally robust co-optimization of P2P energy trading and network operation for interconnected microgrids," *IEEE Trans. Smart Grid*, vol. 12, no. 6, pp. 5172–5184, Nov. 2021.
[13] Y. Wang, Z. Huang, Z. Li, X. Wu, L. L. Lai, and F. Xu, "Transactive energy trading in reconfigurable multi-carrier energy systems," *J. Modern Power Syst. Clean Energy*, vol. 8, no. 1, pp. 67–76, Jan. 2020, doi: 10.35833/mpce.2018.000832.
[14] N. Liu, L. Zhou, C. Wang, X. Yu, and X. Ma, "Heat-electricity coupled peak load shifting for multi-energy industrial parks: A Stackelberg game approach," *IEEE Trans. Sustain. Energy*, vol. 11, no. 3, pp. 1858–1869, Jul. 2020.
[15] A. Fleischhacker, H. Auer, G. Lettner, and A. Botterud, "Sharing solar PV and energy storage in apartment buildings: Resource allocation and pricing," *IEEE Trans. Smart Grid*, vol. 10, no. 4, pp. 3963–3973, Jul. 2019, doi: 10.1109/tsg.2018.2844877.
[16] Q. Peng et al., "Hybrid energy sharing mechanism for integrated energy systems based on the Stackelberg game," *CSEE J. Power Energy Syst.*, vol. 7, no. 5, pp. 911–921, Sep. 2021.
[17] A. Ali, N. Liu, and L. He, "Multi-party energy management and economics of integrated energy microgrid with PV/T and combined heat and power system," *IET Renewable Power Gener.*, vol. 13, no. 3, pp. 451–461, 2019.
[18] X. Zhu et al., "Day-ahead energy pricing and management method for regional integrated energy systems considering multi-energy demand responses," *Energy*, vol. 251, 2022, Art. no. 123914.
[19] E. Nasrolahpour, J. Kazempour, H. Zareipour, and W. D. Rosehart, "A bilevel model for participation of a storage system in energy and reserve markets," *IEEE Trans. Sustain. Energy*, vol. 9, no. 2, pp. 582–598, Apr. 2018, doi: 10.1109/tste.2017.2749434.
[20] Y. Zou, Y. Xu, X. Feng, R. Naayagi, and B.-H. Soong, "Transactive energy system in active distribution networks: A comprehensive review," *CSEE J. Power Energy Syst.*, vol. 8, no. 5, pp. 1302–1317, Sep. 2022.
[21] Z. Li, Y. Xu, S. Fang, X. Zheng, and X. Feng, "Robust coordination of a hybrid AC/DC multi-energy ship microgrid with flexible voyage and thermal loads," *IEEE Trans. Smart Grid*, vol. 11, no. 4, pp. 2782–2793, Jul. 2020, doi: 10.1109/tsg.2020.2964831.
[22] Y. Jiang, C. Wan, C. Chen, M. Shahidehpour, and Y. Song, "A hybrid stochastic-interval operation strategy for multi-energy microgrids," *IEEE Trans. Smart Grid*, vol. 11, no. 1, pp. 440–456, Jan. 2020.
[23] J. Tan, Q. Wu, M. Zhang, W. Wei, F. Liu, and B. Pan, "Chance-constrained energy and multi-type reserves scheduling exploiting flexibility from combined power and heat units and heat pumps," *Energy*, vol. 233, 2021, Art. no. 121176.
[24] M. Daneshvar, B. Mohammadi-Ivatloo, K. Zare, and S. Asadi, "Two-stage robust stochastic model scheduling for transactive energy based renewable microgrids," *IEEE Trans. Ind. Inform.*, vol. 16, no. 11, pp. 6857–6867, Nov. 2020.
[25] H. Von Stackelberg, *Market Structure and Equilibrium*. Berlin, Germany: Springer, 2010.
[26] J. Li, C. Zhang, Z. Xu, J. Wang, J. Zhao, and Y.-J. A. Zhang, "Distributed transactive energy trading framework in distribution networks," *IEEE Trans. Power Syst.*, vol. 33, no. 6, pp. 7215–7227, Nov. 2018, doi: 10.1109/tpwrs.2018.2854649.
[27] S. Boyd and L. Vandenberghe, *Convex Optimization*. Cambridge, U.K.: Cambridge Univ. Press, 2004.
[28] C. Ruiz, A. J. Conejo, and S. A. Gabriel, "Pricing non-convexities in an electricity pool," *IEEE Trans. Power Syst.*, vol. 27, no. 3, pp. 1334–1342, Aug. 2012.
[29] Y. Xu, Z. Y. Dong, R. Zhang, and D. J. Hill, "Multi-timescale coordinated voltage/var control of high renewable-penetrated distribution systems," *IEEE Trans. Power Syst.*, vol. 32, no. 6, pp. 4398–4408, Nov. 2017.
[30] E. Grass, K. Fischer, and A. Rams, "An accelerated L-shaped method for solving two-stage stochastic programs in disaster management," *Ann. Operations Res.*, vol. 284, no. 2, pp. 557–582, 2020.
[31] P. Xiong and P. Jirutitijaroen, "Stochastic unit commitment using multi-cut decomposition algorithm with partial aggregation," in *Proc. IEEE Power Energy Soc. Gen. Meeting*, 2011, pp. 1–8.
[32] C. C. Carøe and R. Schultz, "Dual decomposition in stochastic integer programming," *Operations Res. Lett.*, vol. 24, no. 1-2, pp. 37–45, 1999.
[33] A. Arif, Z. Wang, C. Chen, and B. Chen, "A stochastic multi-commodity logistic model for disaster preparation in distribution systems," *IEEE Trans. Smart Grid*, vol. 11, no. 1, pp. 565–576, Jan. 2020.
[34] V. Kaisermayer, D. Muschick, M. Horn, and M. Gölles, "Progressive hedging for stochastic energy management systems," *Energy Syst.*, vol. 12, no. 1, pp. 1–29, 2021.
[35] S. Boyd, N. Parikh, E. Chu, B. Peleato, and J. Eckstein, "Distributed optimization and statistical learning via the alternating direction method of multipliers," *Found. Trends Mach. Learn.*, vol. 3, no. 1, pp. 1–122, 2011.
[36] D. Bertsimas, E. Litvinov, X. A. Sun, J. Zhao, and T. Zheng, "Adaptive robust optimization for the security constrained unit commitment problem," *IEEE Trans. Power Syst.*, vol. 28, no. 1, pp. 52–63, Feb. 2013.
[37] "Appendices of MEMG energy management," 2022. [Online]. Available: https://www.dropbox.com/s/3w9oxwp1d7vf7tu/MEMG_TEM_Appendices.pdf?dl=0

Yunyang Zou (Student Member, IEEE) received the B.E. and M.E. degrees from Zhejiang University, Hangzhou, China, in 2014 and 2017, respectively. He is currently working toward the Ph.D. degree with the School of Electrical and Electronic Engineering, Nanyang Technological University, Singapore. His research interests include renewable energy integration, energy management, microgrid and multi-energy system operation, and energy transactions.

Yan Xu (Senior Member, IEEE) received the B.E. and M.E. degrees from South China University of Technology, Guangzhou, China, in 2008 and 2011, respectively, and the Ph.D. degree from The University of Newcastle, Callaghan NSW, Australia, in 2013. He conducted Postdoctoral Research with the University of Sydney Postdoctoral Fellowship, and then joined Nanyang Technological University with The Nanyang Assistant Professorship. He is currently an Associate Professor with the School of Electrical and Electronic Engineering and a Cluster Director with Energy Research Institute @ NTU (ERI@N). His research interests include power system stability and control, microgrid, and data-analytics for smart grid applications. Dr. Xu is the Editor of IEEE TRANSACTIONS SMART GRID, and IEEE TRANSACTIONS POWER SYSTEMS. He is also the Chairman of IEEE Power and Energy Society Singapore Chapter.

Cuo Zhang (Member IEEE) received the B.E. (Hons.) degree in electrical (power) engineering from the University of Sydney, Camperdown, NSW, Australia, in 2014, and the Ph.D. degree in electrical engineering from the University of New South Wales, Sydney, NSW, Australia, in 2018. He is currently a Lecturer of power engineering with the University of Sydney. His research interests include power system planning and operation, voltage stability and control, transactive energy, distributed energy resources, microgrids, multi-energy systems, and applications of optimization theory and artificial intelligence in these areas. He was the recipient of 2021 IEEE Transactions Smart Grid Outstanding Paper, two IEEE PES General Meeting Best Conference Papers, UNSW Promoting High Quality Research Papers Scheme Award, and University Medal from the University of Sydney.